

# Storm track processes and the opposing influences of climate change

T. A. Shaw<sup>1\*</sup>, M. Baldwin<sup>2</sup>, E. A. Barnes<sup>3</sup>, R. Caballero<sup>4,5</sup>, C. I. Garfinkel<sup>6</sup>, Y.-T. Hwang<sup>7</sup>, C. Li<sup>8,9</sup>, P. A. O’Gorman<sup>10</sup>, G. Rivière<sup>11</sup>, I. R. Simpson<sup>12</sup> and A. Voigt<sup>13</sup>

**Extratropical cyclones are storm systems that are observed to travel preferentially within confined regions known as storm tracks. They contribute to precipitation, wind and temperature extremes in mid-latitudes. Cyclones tend to form where surface temperature gradients are large, and the jet stream influences their speed and direction of travel. Storm tracks shape the global climate through transport of energy and momentum. The intensity and location of storm tracks varies seasonally, and in response to other natural variations, such as changes in tropical sea surface temperature. A hierarchy of numerical models of the atmosphere–ocean system — from highly idealized to comprehensive — has been used to study and predict responses of storm tracks to anthropogenic climate change. The future position and intensity of storm tracks depend on processes that alter temperature gradients. However, different processes can have opposing influences on temperature gradients, which leads to a tug of war on storm track responses and makes future projections more difficult. For example, as climate warms, surface short-wave cloud radiative changes increase the Equator-to-pole temperature gradient, but at the same time, longwave cloud radiative changes reduce this gradient. Future progress depends on understanding and accurately quantifying the relative influence of such processes on the storm tracks.**

Storm tracks are identified as regions where extratropical cyclones are statistically most common in the mid-latitudes (~30–60° latitude)<sup>1,2</sup>, that is, the North Atlantic, North Pacific and Southern oceans, and the Mediterranean Sea (Fig. 1a). We exclude tropical cyclones (hurricanes and typhoons) and herein we use the term cyclones to refer to extratropical cyclones. Cyclones are typically defined as the region surrounding a local minimum in sea level pressure. In contrast, anticyclones are defined as local maxima in sea level pressure. Eddies are deviations from the time or longitudinally averaged flow and thus include both cyclones and anticyclones. Storm tracks commonly refer to the collective surface tracks of individual cyclones (blue lines in Fig. 1a). Other metrics can be used to define storm tracks, including regions with large eddy kinetic energy (EKE, colour contours in Fig. 1a), heat and momentum transports, or surface pressure variance, where these quantities are calculated using winds, temperature and pressure filtered to retain short timescales (for example, less than 10 days)<sup>3</sup>.

Local weather in mid-latitudes is shaped by cyclones. Most precipitation extremes over the mid-latitudes occur in cyclones and their associated fronts and warm conveyor belts (WCBs)<sup>4,5</sup> (Fig. 2). WCBs are trajectories of moist air parcels near the surface ahead of cold fronts that experience rapid slantwise ascent with latent heat release (Box 1). WCBs and precipitation extremes are strongly linked over the mid-latitude oceans (Fig. 2). Many mid-latitude extreme precipitation events also feature a narrow region

of large, vertically integrated water vapour content that extends equatorward (the so-called atmospheric river)<sup>6</sup>.

Wind extremes are associated with strong cyclones and cause economic losses approximately proportional to the third power of the wind<sup>7</sup>. Some of the strongest near-surface winds are in the WCB region equatorward and to the east of the storm centre<sup>8</sup>. Damaging winds are also caused by sting jets<sup>9</sup> in the dry region of cyclones behind the cold front and in the cold conveyor belt that wraps around the west side of the cyclone. The most destructive wind extremes are not always associated with the most intense pressure anomalies. Large-scale, pre-existing gradients in mean sea level pressure can act to enhance the winds and generate synoptic-scale impacts<sup>10</sup>.

Mid-latitude temperature extremes are associated with warm and cold air advection by strong cyclones. Warm temperature extremes can also result from strong adiabatic warming due to downward motion and radiative anomalies in blocking anticyclones<sup>11–13</sup>. The percentage of blocking-related warm temperature extremes exceeds 80% in large continental regions north of 45° N, and exceeds 60% over the oceans<sup>11</sup>.

Storm tracks are also important because they maintain Earth’s habitable climate by transporting energy poleward (Fig. 1b) thereby reducing the energy imbalance between the Equator and the pole<sup>14</sup>. The poleward energy transport is dominated by enthalpy and potential energy (combined into the so-called dry static energy) and latent energy (moisture) transport. In addition, storm tracks

<sup>1</sup>Department of the Geophysical Sciences, The University of Chicago, Chicago, Illinois 60637, USA. <sup>2</sup>Department of Mathematics, University of Exeter, Exeter EX4 4HQ, UK. <sup>3</sup>Department of Atmospheric Science, Colorado State University, Fort Collins, Colorado 80923, USA. <sup>4</sup>Department of Meteorology, Stockholm University, Stockholm 106 91, Sweden. <sup>5</sup>Bolin Centre for Climate Research, Stockholm University, Stockholm 106 91, Sweden. <sup>6</sup>The Fredy and Nadine Herrmann Institute of Earth Sciences, Hebrew University, Jerusalem 91904, Israel. <sup>7</sup>Department of Atmospheric Sciences, National Taiwan University, Taipei 10617, Taiwan. <sup>8</sup>Geophysical Institute, University of Bergen, Bergen 5020, Norway. <sup>9</sup>Bjerknes Centre for Climate Research, University of Bergen, Bergen 5020, Norway. <sup>10</sup>Department of Earth, Atmospheric and Planetary Sciences, Massachusetts Institute of Technology, Cambridge, Massachusetts 02139, USA. <sup>11</sup>Laboratoire de Meteorologie Dynamique/IPSL, Ecole Normale Supérieure/CNRS, Paris 75006, France. <sup>12</sup>National Center for Atmospheric Research, Boulder, Colorado 80305, USA. <sup>13</sup>Lamont-Doherty Earth Observatory, Columbia University, New York 10964, USA.

\*e-mail: [tas1@uchicago.edu](mailto:tas1@uchicago.edu)

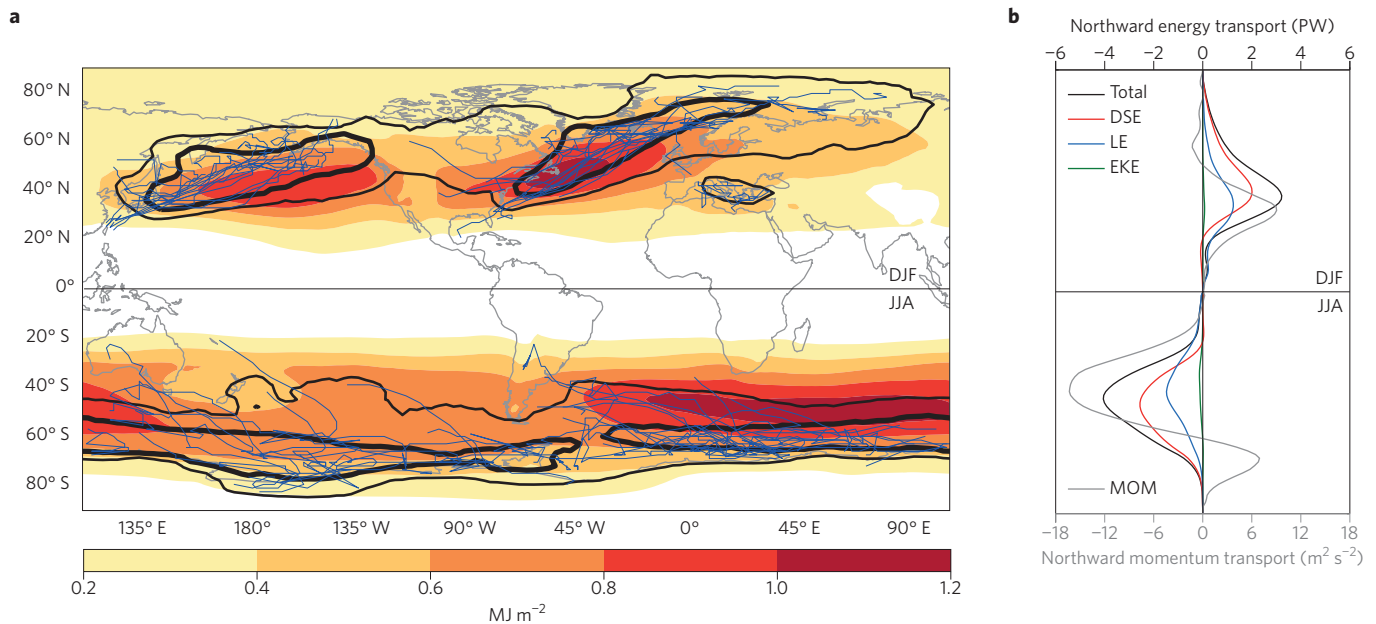


**Figure 1 | Wintertime (December–February, DJF, in the Northern Hemisphere and June–August, JJA, in the Southern Hemisphere) storm tracks.**

**a**, Vertically averaged, ten-day high-pass filtered EKE from ERA-Interim reanalysis data set (see Methods; coloured shading). Black contours show cyclone track density defined following ref. 100 (see Methods); thin contour, 10 tracks (10<sup>6</sup> km<sup>2</sup>)<sup>-1</sup> per season; thick contour, 20 tracks (10<sup>6</sup> km<sup>2</sup>)<sup>-1</sup> per season. Blue lines show individual cyclone tracks for the top 0.5% most intense cyclones ranked by minimum sea-level pressure (shown separately for the Pacific, North Atlantic, Mediterranean and Southern Oceans). **b**, Vertically and longitudinally averaged, ten-day high-pass filtered, northward total energy transport (black) and momentum transport (MOM; grey) from ERA-Interim. Energy transport is divided into dry static energy (DSE; red), latent energy (LE; blue) and EKE (green).

converge momentum in mid-latitudes, thereby maintaining the surface westerlies against surface friction<sup>15</sup> (Fig. 1b).

Owing to the combined importance of storm tracks for weather and climate, one of the most pressing questions in climate research is “how will the storm tracks respond to anthropogenic climate change?”<sup>16</sup>. Here, we review recent progress towards answering this question by summarizing our understanding of storm track processes, including the factors that determine their location, intensity and variability. We highlight a prominent approach for studying storm track processes and their response to climate change, namely the use of a hierarchy of models of varying physical complexity. Finally, we discuss the present understanding of the storm track response to climate change and highlight the opposing influences that thermodynamic responses can have on the storm tracks.

### Existence of storm tracks

Storm tracks are regions within which cyclones preferentially generate, propagate and dissipate, and where energy and momentum transport are largest in mid-latitudes. Fundamentally, cyclones exist due to baroclinic instability, a fluid dynamical instability characteristic of rotating, stratified fluids<sup>17</sup>. Baroclinic instability requires a horizontal temperature gradient, created by differential solar heating that makes the Equator warmer than the poles, and planetary rotation. Baroclinic instability converts potential energy stored in a longitudinal average of such a fluid into the kinetic energy of growing longitudinally dependent perturbations, that is, trains of cyclones and anticyclones or eddies<sup>3,15</sup>.

Our understanding of the processes generating cyclones and storm tracks is encapsulated in a hierarchy of models with increasing physical complexity (Box 2). The most complex models are compared with observational products. The important physical concepts underlying baroclinic instability can be conceptualized in the so-called two-layer quasi-geostrophic (QG) model of the atmosphere. This two-layer model idealizes the atmosphere as two

incompressible, dry ideal gas layers representing the lower and upper troposphere. The fluid flow is taken to be in hydrostatic (a force balance between gravitational acceleration and vertical pressure gradient) and geostrophic (a force balance between Coriolis acceleration and horizontal pressure gradients) balance. Instability occurs via the vertical shear in the jet stream, which is connected to the imposed horizontal temperature gradient by thermal wind balance. Thermal wind balance is the combined relationship where horizontal temperature gradients balance vertical variations of geostrophic wind in hydrostatic equilibrium.

In the lower troposphere, cyclones grow and develop fronts (Fig. 3). Despite their simplicity, QG theories give a reasonable prediction for the propagation speed and length scale of cyclones. A commonly used measure of baroclinicity (when the gradient of pressure and the gradient of density are not aligned) is the maximum Eady growth rate. The Eady growth rate is proportional to the Equator-to-pole temperature gradient and inversely proportional to the vertical potential temperature gradient. It gives an estimate of the growth rate of baroclinic instability<sup>18</sup>. For mid-latitude conditions in the troposphere, the most unstable disturbances predicted from this simplified QG model have a wavelength of approximately 4,000 km and a growth rate of 1 d<sup>-1</sup>, consistent with the observed cyclone climatology.

In the upper troposphere, eddies interact with the jet stream, which serves as a wave guide<sup>19</sup>. The theoretical QG phase velocity of the eddies is midway between the low-layer and upper-layer wind speed<sup>20</sup>, which is in reasonable agreement with the observation that the surface cyclones move with a speed proportional to the mid-tropospheric wind. Eddy activity is transferred eastward<sup>21</sup> and upward<sup>22</sup> (white arrows with dashed outline in Fig. 3). The upward transfer is connected to the westward phase ‘tilt-with-height’ of individual cyclones.

Eddies propagate away from regions of surface baroclinicity towards the subtropics and poles, thereby converging eastward

momentum in mid-latitudes (horizontal white arrows with black outline, right vertical panel of Fig. 3). This eastward momentum convergence maintains an eddy-driven jet stream with surface westerlies (white shading, right vertical panel of Fig. 3) against surface friction. The decay of eddies occurs mainly through kinetic energy transfer from eddies to the jet stream in the upper troposphere, and through mechanical dissipation at the surface<sup>3</sup>. Eddy-jet interactions in the upper layer can be studied in isolation using single-layer shallow-water models with stochastic forcing<sup>23</sup> (Box 2). Although the simplified two-layer QG model illustrates the important dynamics of baroclinic instability, it does not capture the full range of physical processes. Extending theories to fully include moist processes (Box 1) is an important area of research at present.

The growth, development and decay of individual cyclones exhibit significant variability<sup>24</sup>, and the time average of this behaviour manifests as storm tracks. The potential to kinetic energy conversion during the cyclone lifecycle is accompanied by poleward energy transport. This poleward energy transport can be parameterized as a diffusive down-gradient process where the diffusivity is related to the eddy amplitude<sup>25</sup>. The poleward energy transport within storm tracks reduces the Equator-to-pole energy gradient, thereby stabilizing the mean state<sup>15</sup>. Thus, to maintain an active storm track, the Equator-to-pole gradient must be continually restored. There is a continual competition between storm track energy transport, which reduces the Equator-to-pole energy gradient, and restoring mechanisms that act to enhance the gradient, for example, radiative forcing associated with solar insolation, and moist processes within storm tracks<sup>26</sup> (Box 1). Longitudinal surface asymmetries and quasi-stationary high and low pressure patterns or stationary eddies also help to maintain regional horizontal temperature gradients (see below).

Cyclones and storm tracks exist because of baroclinic instability, which is affected by both the Equator-to-pole temperature gradient and the vertical potential temperature gradient. Thus, horizontal and vertical temperature gradients are key variables determining the strength and frequency of storms within the storm tracks and the poleward energy transport across the storm tracks.

### Location, intensity and temporal variability

One primary factor affecting the location and intensity of storm tracks is the seasonality of insolation. Storm tracks generally reach maximum intensity (for example, largest number of cyclones) during winter when surface baroclinicity is strongest, and minimum intensity during summer when baroclinicity is weakest<sup>3</sup>. (The notable exception is the Pacific storm track, whose intensity drops in mid-winter in spite of strong baroclinicity<sup>3</sup>.) Consistently, poleward energy transport by storm tracks is largest during winter and weakest during summer<sup>14</sup>. The winter to summer intensity changes coincide with a poleward shift of storm tracks<sup>3</sup> and jet streams<sup>27</sup> in the Northern Hemisphere.

Seasonal changes in baroclinicity are mediated by the tropical Hadley circulation (the mass circulation in the tropics that involves air rising near the Equator and sinking in the subtropics). Energy transport by the Hadley circulation weakens tropical meridional temperature gradients and enhances baroclinicity in the subtropics, especially in the winter hemisphere<sup>28</sup>. In the upper troposphere, angular momentum transport by the Hadley circulation drives a subtropical jet stream that is strongest in the winter hemisphere<sup>15</sup>. As noted above, storm track processes in the upper troposphere drive a separate, eddy-driven jet poleward of the subtropical jet<sup>15</sup>. The interaction between the subtropical and eddy-driven jets has been studied using idealized dry dynamical core models with simplified boundary conditions (Box 2). If the Hadley circulation is strong and mid-latitude baroclinicity is weak, the storm tracks lie close to the subtropics and there is a single jet, whereas weakening of the Hadley circulation and/or strengthening mid-latitude

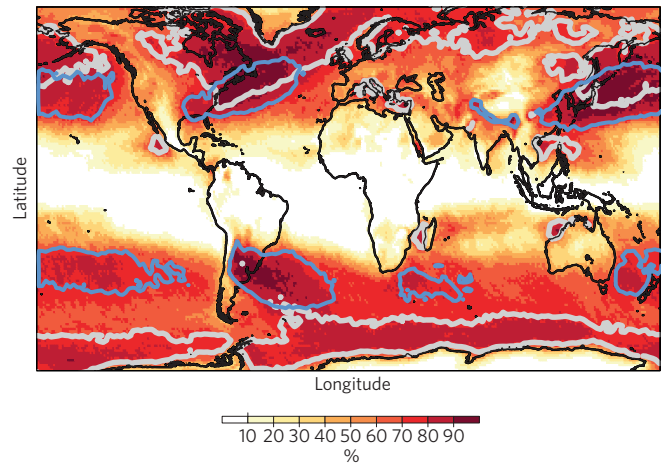


**Figure 2 | Mid-latitude precipitation extremes associated with storm tracks.** Percentage of extreme precipitation events (coloured shading) associated with either a cyclone (defined as the region surrounding an area of low pressure) or a WCB. Contours indicate areas where 70% of the extreme events are related to a cyclone (light grey contour) or a WCB (blue contour). Results are based on ERA-Interim reanalysis data for 1979–2010 and extreme events are defined as the top 1% of six-hourly precipitation rates at each grid point. Figure reproduced with permission from ref. 4, AMS.

baroclinicity will lead to a poleward shift of the storm tracks and a double jet<sup>29,30</sup>. The idealized model relationships seem to hold in the real world: for example, when comparing the Pacific (equatorward storm track, single jet) against the Atlantic (poleward storm track, multiple separated jets) sectors<sup>31</sup>.

The time-mean position and intensity of mid-latitude storm tracks are also strongly influenced by the boundaries that surround them: the underlying surface, which forms the lower boundary to the atmosphere, as well as the overlying stratosphere, and the tropical and polar atmosphere on either side. Warm ocean boundary currents enhance baroclinicity locally<sup>32</sup> and their impact can be detected in high-resolution observations and modelling<sup>33</sup>. Cyclones within the storm tracks amplify as they pass through these regions of enhanced baroclinicity<sup>3</sup>. Atmospheric stationary eddies generated by warm ocean boundary currents tend to destroy baroclinicity downstream<sup>34</sup> and dissipation occurs over the continents. Both of these factors limit the longitudinal extent of storm tracks. Surface orography also generates stationary eddies<sup>35</sup>. During wintertime, stationary eddies couple with the stratosphere: this affects the north–south position of the Atlantic storm track<sup>36</sup>. Differences in surface conditions account for the very different longitudinal structure and seasonal cycle of storm tracks in the Northern and Southern hemispheres<sup>3</sup>. Models with realistic surface boundary conditions simulate realistic longitudinally confined storm tracks in the ocean basins of the Northern Hemisphere (Box 2).

Observational evidence exists for storm track variations on sub-seasonal to millennial timescales. The most prominent modes of temporal variability in longitudinally averaged statistics (so-called annular modes) occur on a weekly timescale in both hemispheres<sup>37</sup> and involve: (1) a north–south displacement of the eddy-driven jet; and (2) changes in jet intensity. These high-frequency fluctuations arise mostly from nonlinear interactions of eddies and the time- and longitudinally averaged flow. Once the jet is displaced, eddies reinforce the displacement; this positive feedback increases the persistence of fluctuations by up to ten days or more<sup>37</sup>. Variations in storm track intensity are manifest as temporal variability in EKE, eddy heat fluxes and baroclinicity<sup>38</sup>. The balance between diabatic production of baroclinicity and destruction by baroclinic instability can

**Box 1 | Role of moist processes.**

Storm tracks interact with moist processes (water vapour, clouds and precipitation) in two ways: latent heat release and radiation.

**Latent heating.** In the mid-latitudes, latent heating occurs predominantly in the WCB region of cyclones, where warm air moves upward and water vapour condenses. It intensifies the cyclonic circulation<sup>78</sup>, which suggests that increased latent heating in a warmer climate will have a strengthening effect on cyclones. To leading order, the effect of latent heating on eddies may be represented by a reduced mean static stability<sup>79</sup>, but recent results suggest a larger role when small-scale processes are better resolved in models<sup>69</sup>. Latent heating shapes vertical stratification and baroclinicity<sup>26,80</sup>, and latent heat transport by storm tracks contributes approximately half of the poleward energy transport in mid-latitudes<sup>14</sup>. A comprehensive review of the role of latent heating can be found in ref. 80.

**Radiation.** The second way that extratropical cyclones and storm tracks interact with moist processes is via radiation. Cirrus and stratus clouds form during slantwise ascent in the WCB region, whereas cumulus clouds form along the cold front<sup>81,82</sup>. CREs, defined as the difference between clear-sky and all-sky radiation, involve both shortwave and longwave radiation. Shortwave CREs quantify reflection of incoming shortwave radiation by clouds, which cools the surface. Longwave CREs quantify the trapping of outgoing longwave radiation by clouds, which warms the surface. Shortwave CREs dominate at the surface and longwave CREs dominate inside the atmosphere<sup>83</sup>. In models, atmospheric CREs can intensify the jet stream<sup>84,85</sup>. Climate model biases in shortwave CREs over the Southern Ocean may contribute to jet stream biases through their effects on equator-to-pole SST gradients<sup>86</sup>. CREs may also regulate unforced climate variability, for example, by shortening its time-scale<sup>87</sup>. Observations and models both support the idea of a two-way interaction between clouds and storm tracks. For example, latitudinal shifts of storm tracks coincide with shifts of upper tropospheric clouds, which increases outgoing longwave radiation in the region away from which the storm track shifts<sup>86,88</sup>.

Clouds represent a substantial fraction of the uncertainty in modelled climate sensitivity (that is, increase in globally averaged surface temperature due to a doubling of atmospheric CO<sub>2</sub>)<sup>16</sup>. The mid-latitude circulation response to climate change is also uncertain<sup>89</sup>, and there is mounting evidence that the circulation uncertainty is partially linked to the radiative response of clouds<sup>90,91</sup>.

The quantitative impact of cloud radiative changes on the circulation response to global warming can be assessed using the model hierarchy (Box 2) and a technique that suppresses cloud radiative changes by locking the radiative properties of clouds and water vapour to the present climate (the so-called locking method)<sup>90,92</sup>. The application of the locking method to a prescribed-SST aquaplanet model simulation is shown in Fig. B1. Global warming produces a poleward shift of the eddy-driven jet stream. Cloud radiative changes alone contribute roughly half of the total jet stream response in this set-up (see Fig. B1a). The cloud-induced poleward shift of the jet can be understood as the response to radiative forcing caused by cloud changes (see Fig. B1b), isolated using the partial radiative perturbation method<sup>92,97</sup>. In response to cloud radiative changes, heating of the tropical and mid-latitude upper troposphere and cooling of the high-latitude lower troposphere increase static stability and baroclinicity, which are known to shift the jet poleward<sup>52</sup>.

The simulations also reveal a potential tug of war between the impact of longwave and shortwave cloud changes on surface baroclinicity. Cooling induced by shortwave cloud changes (blue line, Fig. B1c), due mostly to cloud microphysical changes, increases surface baroclinicity and would enhance the poleward jet shift. However, warming induced by longwave cloud changes decreases baroclinicity (red line, Fig. B1c). The outcome of the tug of war is unclear and probably model-dependent, suggesting that it might contribute to the uncertainty of the circulation response to increased CO<sub>2</sub>. A better understanding of the two-way interaction between clouds and storm tracks is needed to improve model estimates of future storm track changes<sup>16</sup>. Progress can be made by adding models with simplified representations of cloud processes to the model hierarchy (Box 2).

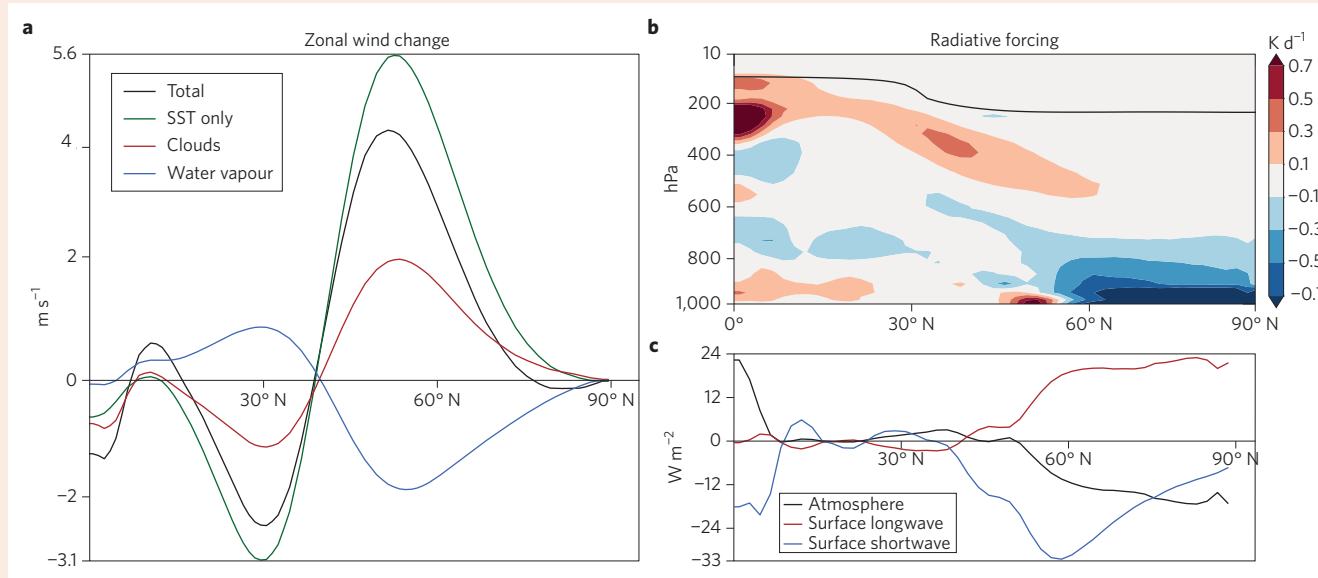


**Figure B1 | Radiative impact of clouds on the jet stream response to global warming in the ECHAM6 aquaplanet model.** **a**, Contributions to the total east-west wind response at 850 hPa (black) from surface warming (green), radiative changes of clouds (red) and water vapour (blue). **b**, Radiative forcing inside the atmosphere due to cloud changes. The tropopause is indicated by the thick black line. **c**, Vertically integrated atmospheric (black) and surface shortwave (blue) and longwave (red) cloud radiative forcing. Figure reproduced with permission from ref. 90, NPG.

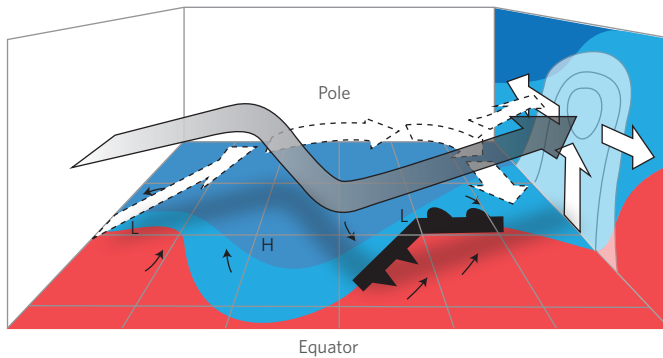


**Figure 3 | Schematic of a storm track.** Surface extratropical cyclone (L; low pressure) and anticyclone (H; high pressure) represent a snapshot of a series of eddies within the storm track. The surface features are coupled to the jet stream in the upper troposphere (indicated by the grey arrow). White vectors with dashed outline indicate the approximate time-averaged eddy propagation through the storm tracks<sup>20</sup>. Eddy activity originates at low levels and propagates eastward and upward. The longitudinally averaged eddy propagation is upward and then poleward/equatorward, converging momentum flux into the jet stream<sup>21</sup>, as indicated by white arrows with solid black outline on the right-hand panel. Figure reproduced with permission from ref. 21, AMS.

explain the oscillating behaviour of baroclinicity and storm track activity<sup>38,39</sup>. These modes of variability are important because they manifest in response to external forcing, for example, in response to anthropogenic forcing (ozone depletion and greenhouse gas changes<sup>40</sup>) and variations in the stratospheric polar vortex<sup>41</sup>.

Tropical climate variability across a range of timescales (for example, sub-seasonal Madden–Julian Oscillation to interannual and decadal El Niño–Southern Oscillation) drives anomalous stationary eddies that propagate into the extratropics and affect the storm tracks<sup>42–44</sup>. Much like the temporal variability discussed above, storm tracks generally exhibit a positive feedback in response to tropically forced stationary eddies<sup>45</sup>. Indeed, a warmer ocean in the warm pool region (red dashed box in Fig. 4a) triggers a stationary eddy response extending into mid-to-high latitudes over North America (shading in Fig. 4b) that is reinforced by high-frequency eddy forcing (contours in Fig. 4b). Interannual and decadal variations in the stratospheric polar vortex and Arctic sea ice can also lead to storm track variability and trends (see recent review articles<sup>41,46</sup>). On geologic timescales, changes in ice sheets and sea ice — for example, during glacial periods — had a profound effect, particularly on the North Atlantic storm track<sup>47</sup>.

### Response to anthropogenic climate change

Owing to anthropogenic activities, the concentration of CO<sub>2</sub> in the atmosphere has increased significantly since pre-industrial times, and is expected to increase further. The response of the storm tracks to increased CO<sub>2</sub> has significant implications for future weather and climate in the mid-latitudes, including for extreme events. Although changes in CO<sub>2</sub> will dominate long-term climate change in mid-latitudes, recent ozone depletion in the Southern Hemisphere has had a significant, detectable impact on the summertime southern storm track. In particular, the jet stream shifted poleward in response to ozone depletion<sup>48</sup>, consistent with predictions of cyclone<sup>49</sup> and storm track<sup>40</sup> changes. Ozone depletion impacts climate via thermodynamics: there is lower stratospheric cooling in the Antarctic (due to reduced ultraviolet warming), which increases upper tropospheric baroclinicity and strengthens the jet stream through thermal wind balance<sup>50</sup>.

A useful starting point for thinking about the storm track response to increased CO<sub>2</sub> is to assess thermodynamic changes that

impact both the Equator-to-pole temperature gradient and the vertical gradient of potential temperature. Global warming has several robust thermodynamic implications. For example: (1) the increase of saturation specific humidity with temperature (via the Clausius–Clapeyron relation) leads to moister low-level air and greater latent heat release in tropical convection, which warms the tropical upper troposphere relative to the surface and raises the tropopause; (2) surface albedo and temperature feedbacks lead to enhanced warming of the Arctic relative to the global mean (Arctic amplification); and (3) increased CO<sub>2</sub> cools the stratosphere by increasing its emissivity<sup>51</sup>. These thermodynamic changes can affect individual cyclones and storm tracks.

Much of our present understanding of the impact of thermodynamic changes in response to increased CO<sub>2</sub> on storm tracks has come through experiments across the model hierarchy (Box 2). The experiments have revealed opposing thermodynamic influences on the storm tracks. For example:

- Dry dynamical core simulations (see Box 2) have shown that warming of the tropical upper troposphere increases baroclinicity and shifts the storm tracks poleward. However, Arctic surface warming decreases lower tropospheric baroclinicity and shifts the storm tracks equatorward<sup>52</sup>. The dry core responses have also been connected to changes in the vertical potential temperature gradient<sup>53</sup> and the Hadley circulation<sup>54</sup>. The competition between Arctic and tropical warming during winter-time<sup>55,56</sup> is reproduced in atmosphere–ocean general circulation models (AOGCMs; see Box 2).
- In AOGCMs, warming of the polar lower stratosphere due to ozone hole recovery decreases baroclinicity and shifts the storm tracks equatorward; however, increased greenhouse gases lead to warming of the tropical upper troposphere, cooling of the lower stratosphere and an opposite storm track shift<sup>40</sup>.
- Latent heat transport increases in mid-latitudes in AOGCMs in response to increased CO<sub>2</sub> consistent with thermodynamic arguments. However, total energy transport does not change by as much because the increased latent energy transport is partially compensated for by decreased dry static energy transport<sup>57,58</sup>.
- In aquaplanet models, changes in the interaction between clouds and shortwave radiation leads to cooling in high latitudes, which increases surface baroclinicity tending to shift storm tracks poleward, whereas longwave cloud changes decrease surface baroclinicity (Box 1).
- Changes in mean available potential energy, which are related to changes in storm track intensity, are sensitive to competition between changes in baroclinicity and vertical stratification<sup>59</sup>.
- Finally, in atmospheric general circulation models (AGCMs; see Box 2), direct radiative forcing (increased CO<sub>2</sub> with fixed sea surface temperatures, SSTs) amplifies summertime stationary eddies and shifts the Pacific storm track poleward. In contrast, the indirect effect of SST warming weakens stationary eddies and shifts the Pacific storm track equatorward<sup>60</sup>.

Taken together, the above examples illustrate the multiple opposing thermodynamic influences that make predicting the storm track response to future climate change challenging. Although the storm tracks are subject to competing thermodynamic influences, the general consensus from comparison of state-of-the-art AOGCM simulations subject to business-as-usual emission scenarios is that the longitudinally averaged eddy-driven jet stream will shift poleward as the climate warms<sup>61</sup>, with associated changes in storm track statistics<sup>62</sup>. In the Northern Hemisphere, the poleward shift is seasonally dependent: it is most robust across models in autumn and is considerably weaker and less robust in winter<sup>61</sup>. These results are consistent with a tug of war on the storm tracks due to opposing thermodynamic changes during winter.

**Box 2 | Idealized modelling framework.**

Storm tracks involve a range of spatial scales from small-scale frontal systems to planetary-scale jet streams. Understanding large-scale, complex systems such as Earth's climate requires a hierarchy of models. The principal idea of the model hierarchy is that complex phenomena can be understood through the study of simpler systems incorporating selected physical processes of the full system<sup>93</sup>. A useful analogy can be made with the field of molecular biology, where an understanding of the human genome is sought through the study of specimens from many taxa of varying complexity (for example, *Escherichia coli* bacteria, *Homo sapiens* and viruses)<sup>93</sup>. The study of storm tracks is built on a hierarchy of models ranging in physical complexity from only the most essential ingredients to state-of-the-art simulations<sup>94</sup>.

QG and shallow water models are at the simple end of the model hierarchy and include the minimal ingredients needed to understand the existence of storm tracks, that is, rotating fluid with horizontal and vertical temperature gradients. QG models form the basis for the theory of baroclinic instability<sup>95</sup>. Single-layer shallow water models with stochastic forcing have been used to study eddy–jet interactions in the upper troposphere<sup>23</sup>.

Dry dynamical core models include full vertical stratification and simplified representation of radiative and convective processes<sup>96</sup>. In the standard configuration, the dry core simulates longitudinally invariant 'dry' storm tracks on a sphere (Fig. B2, bottom left). Dry cores have been used to study the storm track response to temperature gradient perturbations induced by global warming<sup>52</sup>.

Moist processes are important for storm track dynamics (Box 1), for example, about half of the poleward energy transport by storm tracks is via latent heat. Idealized moist core models include the interaction of storms with latent heating and precipitation, but do not include radiative feedbacks and clouds<sup>97,98</sup>. The moisture source is evaporation from an aquaplanet surface (no continents) that can be either prescribed SST or a slab ocean (immovable layer of water of fixed depth and heat capacity).

Aquaplanet models simulate storm tracks including interactions with latent heat, clouds and radiative feedbacks, but retain simplified surface boundary conditions (no continents)<sup>94</sup>. These models simulate precipitating storm tracks (Fig. B2, bottom middle) and allow for the study of the storm track response to changes in SST gradients, global warming and cloud radiative interactions (Box 1). Aquaplanet models coupled to a slab ocean or ocean mixed layer include coupling between storm tracks, cloud radiative interactions and SST.

At the complex end, the Earth AGCM includes realistic land surface boundary conditions with prescribed SST. AOGCM add a dynamic ocean circulation. These models simulate realistic longitudinally confined storm tracks (Fig. B2, bottom right). Although our ability to simulate Earth's weather and climate has improved considerably over the past few decades, today's state-of-the-art climate models still exhibit biases in storm track position and intensity<sup>66</sup>. These biases are probably linked to coarse resolution and the parameterization of small-grid-scale processes such as convection, clouds and boundary layers<sup>99</sup>.

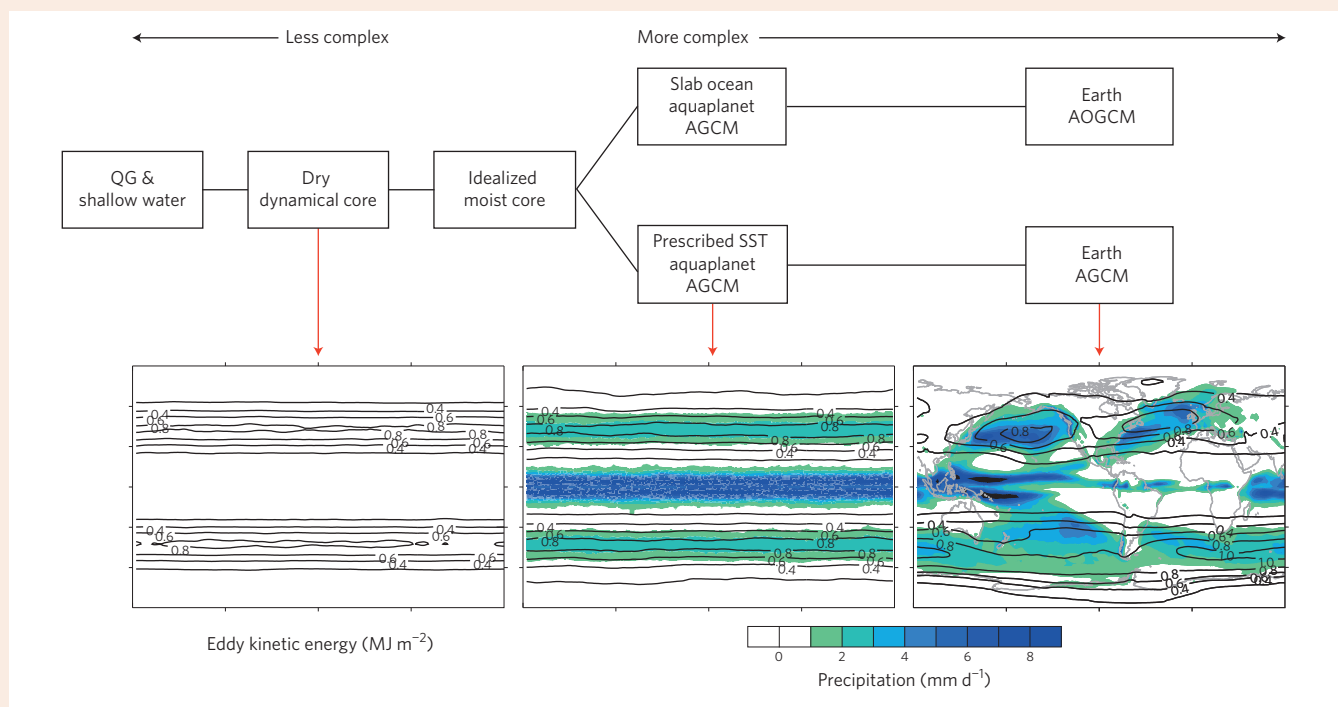


**Figure B2 | Idealized model hierarchy.** Lower panels show examples of modelled vertically integrated EKE (contours) and precipitation (shading). Figure reproduced with permission from ref. 94, MSJ.

Even for aspects of the longitudinally averaged storm track response that are largely agreed on across models, there is considerable inter-model variance in the magnitude of the response. In the Southern Hemisphere, inter-model variance is due equally to uncertainty both in the future temperature trends and in the sensitivity of the circulation<sup>50</sup>. In the North Atlantic, inter-model variance is

mostly due to uncertainty in lower tropospheric Equator-to-pole temperature gradient changes<sup>55</sup>. In addition, today's climate models may overestimate the future response of the longitudinally averaged southern storm tracks because the modelled jet streams are biased equatorward, and eddy-driven jet streams located closer to the Equator may be more sensitive to external forcing<sup>51</sup>.

In the Northern Hemisphere, the predicted storm track response exhibits large deviations from the longitudinal average due to changes in stationary eddies<sup>61</sup>. During Northern Hemisphere summer, the Atlantic jet is predicted to shift poleward, but the Pacific jet exhibits very little change due to the competing effects mentioned above. During winter, changes in stationary eddies lead to a poleward jet shift in the West Pacific and to an equatorward shift in the East Pacific<sup>61</sup>. Accompanying this is a projected increase in extratropical cyclone activity over the west coast of North America<sup>63</sup>. Over the Atlantic basin, the most robust changes are over western Europe, where storm track activity is projected to increase<sup>64</sup>, accompanied by a stationary high pressure response over the Mediterranean<sup>61</sup> and a considerable reduction in Mediterranean storm track activity<sup>64</sup>. Processes that give rise to the regional changes in stationary waves, their connection to extreme events<sup>65</sup> and model biases (for example, the lack of northward tilt of the Atlantic jet<sup>66</sup>) are active areas of research.

Another perspective from which future changes in storm tracks can be viewed is through the change in character of individual cyclones within the storm tracks. Of particular importance when it comes to societal impacts is the change in number, intensity or duration of cyclones. Aquaplanet model simulations show that changes in individual cyclone intensity are subject to competition between baroclinicity changes and increased moisture content of the atmosphere<sup>67</sup>. At present, there is considerable disagreement regarding future changes in the character of individual wintertime cyclones<sup>68</sup>. The disparity between different model studies may be partly due to the wide range of metrics used to characterize intense cyclones. It may also be associated with the net response being a residual of competing thermodynamic changes. The relative importance of these effects in model simulations is likely to depend on model resolution and the representation of small-scale physical processes that are not explicitly resolved by today's global climate models<sup>69</sup>. Improving projections and understanding of future changes in storm intensity is an ongoing topic of research and is likely to evolve with model improvements.

Projected changes in storm track intensity and position in response to climate change over the next century will affect mid-latitude extremes. The dynamical contribution to changes in extratropical precipitation extremes (from changes of vertical winds in storms) can be positive or negative, and is considerably smaller than the thermodynamic contribution related to the increase of saturation specific humidity with warming<sup>70,71</sup>. The dynamical contribution matters more regionally, and the poleward shift of storm tracks impacts precipitation extremes in idealized aquaplanet simulations<sup>72</sup>, but less so in comprehensive simulations<sup>70,71</sup>. A shift towards higher mean temperatures reduces the frequency of temperatures lower than a fixed cold threshold, and increases the frequency of temperatures above a fixed warm threshold<sup>73</sup>. Changes in the intensity of eddies would affect the generation of temperature extremes, but even if wind anomalies do not change in magnitude, warm and cold air advection will be less efficient at generating temperature extremes because of a projected reduction in the surface Equator-to-pole temperature gradient in the Northern Hemisphere<sup>74</sup>. Wind extremes are also sensitive to changes in the wind's mean and variance: changes in storm intensity impact wind variance, and a strengthening of the climatological westerlies (as is projected to occur on the poleward flank of most storm tracks<sup>61</sup>) would lead to more extreme winds<sup>75</sup>. The response to climate change may also project onto large-scale modes of storm track variability, which influence the occurrence of wind, precipitation and temperature extremes by modifying the latitude and intensity of the jet, cyclones and blocking anticyclones<sup>68,73</sup>.

Thermodynamic responses to global warming lead to opposing influences on baroclinicity. Future changes in storm tracks and cyclones may ultimately be determined by how the competing

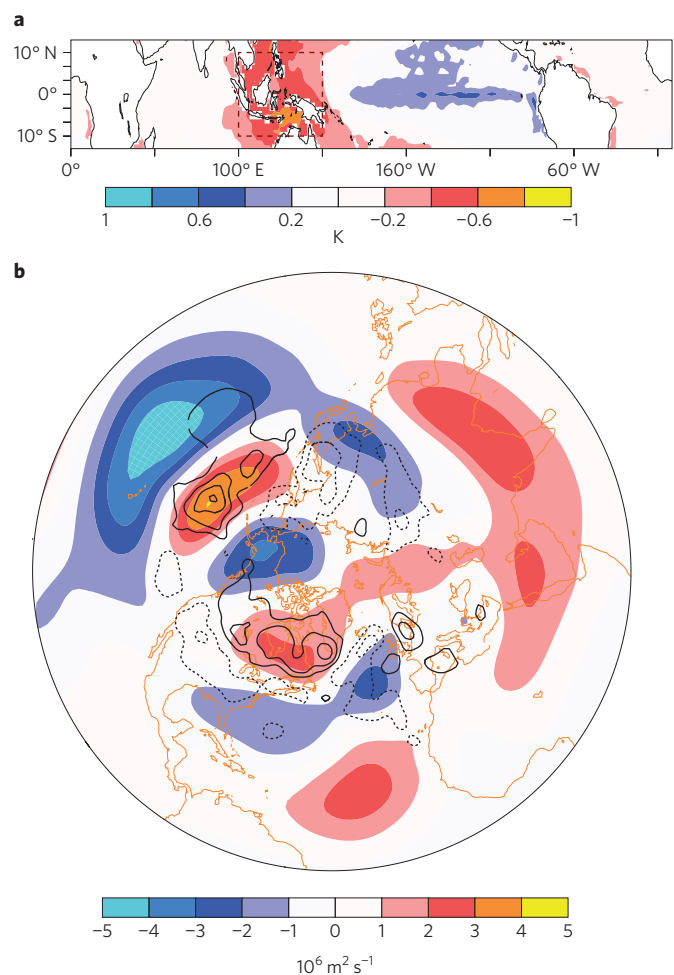


**Figure 4 | Coupling between tropical Pacific SST and the storm track.**

**a**, Anomalous SST at day 0. Daily mean composites of 103 cases of SST values averaged in the West Pacific (dashed red box) exceeding one standard deviation (day 0). **b**, The 300 hPa anomalous stream function (shadings;  $\text{m}^2 \text{s}^{-1}$ ) and the transient eddy feedback, that is, stream function tendency due to the high frequency transients (contours, interval  $3 \text{ m}^2 \text{ s}^{-2}$ , dashed negative) averaged between days 0 and +7.

thermodynamic effects combine transiently. In addition to the thermodynamic tug of war, large internal variability in the mid-latitudes will continue to make the detection and attribution of storm track responses to anthropogenic climate change difficult<sup>76</sup>.

### Opportunities for future research

Nature changes in storm tracks are uncertain because of competing thermodynamic responses to anthropogenic radiative forcing, including changes in  $\text{CO}_2$  and ozone. A promising direction is to constrain the influence of future competing thermodynamic responses by exploiting relationships between modelled future changes and seasonal and interannual variations (so-called emergent constraints)<sup>77</sup>. In addition, synthesizing the storm track response to climate change into a feedback framework — similar to that for the thermodynamic response<sup>16</sup> — by separately quantifying the forcing (changes in baroclinicity) and feedbacks may be a path forward for integrating our understanding of the link between thermodynamics and dynamics.

Overall, progress in our understanding of storm tracks and their response to climate change depends on: (1) additional observations; and (2) filling gaps in the model hierarchy. Additional observations of cyclones are needed to better characterize how moist processes

affect storm tracks and to develop better parameterizations for climate models. This should be combined with additional analysis of storm track changes in response to recent (for example, ozone depletion) and past (for example, glacial–interglacial, past warm climates) forcings. Important gaps exist in the model hierarchy, in particular in terms of cloud processes and their coupling with the circulation. A model with simplified representation of the coupling between storm tracks and cloud radiative effects is needed to further our understanding of the role of clouds in past, present and future climates. All of these complementary studies are required to reduce uncertainties of storm track response to climate change.

## Methods

Methods and any associated references are available in the [online version of the paper](#).

Received 29 December 2015; accepted 6 July 2016;  
published online 29 August 2016

## References

- Hoskins, B. J. & Hodges, K. New perspectives on the Northern Hemisphere winter storm tracks. *J. Atmos. Sci.* **59**, 1041–1061 (2002).
- Hoskins, B. J. & Hodges, K. A new perspective on Southern Hemisphere storm tracks. *J. Clim.* **18**, 4108–4129 (2005).
- Chang, K. M., Lee, S. & Swanson, K. L. Storm track dynamics. *J. Clim.* **15**, 2163–2183 (2002).
- Pfahl, S., Madonna, E., Boettcher, M., Joos, H. & Wernli, H. Warm conveyor belts in the ERA-Interim dataset (1979–2010). Part II: Moisture origin and relevance for precipitation. *J. Clim.* **27**, 27–40 (2014).
- Catto, J. L. & Pfahl, S. The importance of fronts for extreme precipitation. *J. Geophys. Res. Atmos.* **118**, 10791–10801 (2013).
- Dacre, H. F., Clark, P. A., Martinez-Alvarado, O., Stringer, M. A. & Lavers, D. A. How do atmospheric rivers form? *Bull. Am. Meteorol. Soc.* **96**, 1243–1255 (2015).
- Roberts, J. F. *et al.* The XWS open access catalogue of extreme European windstorms from 1979 to 2012. *Nat. Hazards Earth Syst. Sci.* **14**, 2487–2501 (2014).
- Catto, J. L., Shaffrey, L. C. & Hodges, K. I. Can climate models capture the structure of extratropical cyclones? *J. Clim.* **23**, 1621–1635 (2010).
- Baker, L. H., Gray, S. L. & Clark, P. Idealised simulations of sting-jet cyclones. *Q. J. R. Meteorol. Soc.* **140**, 96–110 (2014).
- Fink, A. H., Brucher, T., Ermert, V., Kruger, A. & Pinto, J. G. The European storm Kyrill in January 2007: synoptic evolution, meteorological impacts and some considerations with respect to climate change. *Nat. Hazards Earth Syst. Sci.* **9**, 405–423 (2009).
- Pfahl, S. & Wernli, H. Quantifying the relevance of atmospheric blocking for co-located temperature extremes in the Northern Hemisphere on (sub-)daily time scales. *Geophys. Res. Lett.* **39**, L12807 (2012).
- Bieli, M., Pfahl, S. & Wernli, H. A Lagrangian investigation of hot and cold temperature extremes in Europe. *Q. J. R. Meteorol. Soc.* **141**, 98–108 (2015).
- Loikith, P. C. & Broccoli, A. J. Characteristics of observed atmospheric circulation patterns associated with temperature extremes over North America. *J. Clim.* **25**, 7266–7281 (2012).
- Trenberth, K. E. & Stepaniak, D. P. Covariability of poleward atmospheric energy transports on seasonal and interannual timescales. *J. Clim.* **16**, 3691–3705 (2003).
- Schneider, T. The general circulation of the atmosphere. *Annu. Rev. Earth Planet. Sci.* **34**, 655–688 (2006).
- Bony, S. *et al.* Clouds, circulation and climate sensitivity. *Nat. Geosci.* **8**, 261–268 (2015).
- Grotjahn, R. in *Encyclopedia of Atmospheric Sciences* (eds Holton, J. R., Pyle, J. & Curry, J. A.) 179–188 (Academic, 2003).
- Eady, E. Long waves and cyclone waves. *Tellus* **1**, 33–52 (1949).
- Hoskins, B. J. & Ambrizzi, T. Rossby wave propagation on a realistic longitudinally varying flow. *J. Atmos. Sci.* **50**, 1661–1671 (1993).
- Sanders, F. Analytic solutions of the non-linear omega and vorticity equation for a structurally simple model of disturbances in the baroclinic westerlies. *Mon. Weath. Rev.* **99**, 393–407 (1971).
- Hoskins, B. J., James, I. N. & White, G. H. The shape, propagation and mean-flow interaction of large-scale weather systems. *J. Atmos. Sci.* **40**, 1595–1612 (1983).
- Edmon, H. J., Hoskins, B. J. & McIntyre, M. E. Eliassen–Palm cross sections for the troposphere. *J. Atmos. Sci.* **37**, 2600–2616 (1980).
- Vallis, G. K., Gerber, E. P., Kushner, P. J. & Cash, B. A. A mechanism and simple dynamical model of the North Atlantic Oscillation and annular modes. *J. Atmos. Sci.* **61**, 264–280 (2004).
- Davies, H. C., Schär, C. & Wernli, H. The palette of fronts and cyclones within a baroclinic wave development. *J. Atmos. Sci.* **48**, 1666–1689 (1991).
- Kushner, P. J. & Held, I. M. A test using atmospheric data, of a method for estimating oceanic eddy diffusivity. *Geophys. Res. Lett.* **47**, 4213–4216 (1998).
- Hoskins, B. J. & Valdes, P. J. On the existence of storm tracks. *J. Atmos. Sci.* **47**, 1854–1864 (1990).
- Shaw, T. A. On the role of planetary-scale waves in the abrupt seasonal transition of the Northern Hemisphere general circulation. *J. Atmos. Sci.* **71**, 1724–1746 (2014).
- Lindzen, R. S. & Hou, A. V. Hadley circulations for zonally averaged heating centered off the Equator. *J. Atmos. Sci.* **45**, 2416–2427 (1988).
- Son, S.-W. & Lee, S. The response of westerly jets to thermal driving in a primitive equation model. *J. Atmos. Sci.* **62**, 3741–3757 (2005).
- Brayshaw, D. J., Hoskins, B. & Blackburn, M. The storm-track response to idealized SST perturbations in an aquaplanet GCM. *J. Atmos. Sci.* **65**, 2842–2860 (2008).
- Li, C. & Wettstein, J. J. Thermally driven and eddy-driven jet variability in reanalysis. *J. Clim.* **25**, 1587–1596 (2012).
- Nakamura, H., Sampe, T., Goto, A., Ohfuchi, W. & Xie, S.-P. On the importance of midlatitude oceanic frontal zones for the mean state and dominant variability in the tropospheric circulation. *Geophys. Res. Lett.* **35**, L15709 (2008).
- Czaja, A. & Blunt, N. A new mechanism for ocean–atmosphere coupling in midlatitudes. *Q. J. R. Meteorol. Soc.* **137**, 1095–1101 (2011).
- Kaspi, Y. & Schneider, T. The role of stationary eddies in shaping midlatitude storm tracks. *J. Atmos. Sci.* **70**, 2596–2613 (2013).
- Held, I., Ting, M. & Wang, H. Northern winter stationary waves: theory and modeling. *J. Clim.* **15**, 2125–2144 (2002).
- Shaw, T. A., Perlwitz, J. & Weiner, O. Troposphere–stratosphere coupling: links to North Atlantic weather and climate, including their representation in CMIP5 models. *J. Geophys. Res.-Atmos.* **119**, 5864–5880 (2014).
- Hartmann, D. L. The atmospheric general circulation and its variability. *J. Meteorol. Soc. Jpn* **85**, 123–143 (2007).
- Thompson, D. W. & Barnes, E. A. Periodic variability in the large-scale Southern Hemisphere atmospheric circulation. *Science* **343**, 641–645 (2014).
- Ambaum, M. H. & Novak, L. A nonlinear oscillator describing storm track variability. *Q. J. R. Meteorol. Soc.* **140**, 2680–2684 (2014).
- Thompson, D. W. J. *et al.* Signatures of the Antarctic ozone hole in Southern Hemisphere surface climate change. *Nature Geosci.* **4**, 741–749 (2011).
- Kidston, J. *et al.* Stratospheric influence on tropospheric jet streams, storm tracks and surface weather. *Nature Geosci.* **8**, 433–440 (2015).
- Palmer, T. N. & Mansfield, D. A. Response of two atmospheric general circulation models to sea-surface temperature anomalies in the tropical East and West Pacific. *Nature* **310**, 483–485 (1984).
- Cassou, C. Intraseasonal interaction between the Madden–Julian Oscillation and the North Atlantic Oscillation. *Nature* **455**, 523–527 (2008).
- Baggett, C. & Lee, S. Arctic warming induced by tropically forced tapping of available potential energy and the role of the planetary-scale waves. *J. Atmos. Sci.* **72**, 1562–1568 (2015).
- Drouard, M., Rivière, G. & Arbogast, P. The link between the North Pacific climate variability and the North Atlantic Oscillation via downstream propagation of synoptic waves. *J. Clim.* **28**, 3957–3976 (2015).
- Barnes, E. A. & Screen, J. A. The impact of Arctic warming on the midlatitude jet-stream: Can it? Has it? Will it? *Wiley Interdiscip. Rev. Clim. Change* **6**, 277–286 (2015).
- Merz, N., Raible, C. C. & Woollings, T. North Atlantic eddy-driven jet in interglacial and glacial winter climates. *J. Clim.* **28**, 3977–3997 (2015).
- Lee, S. & Feldstein, S. B. Detecting ozone- and greenhouse gas-driven wind trends with observational data. *Science* **339**, 563–567 (2013).
- Grise, K. M., Son, S.-W., Correa, G. J. P. & Polyani, L. M. The response of extratropical cyclones in the Southern Hemisphere to stratospheric ozone depletion in the 20th century. *Atmos. Sci. Lett.* **15**, 29–36 (2014).
- Gerber, E. P. & Son, S.-W. Quantifying the summertime response of the austral jet stream and Hadley cell to stratospheric ozone and greenhouse gases. *J. Atmos. Sci.* **71**, 5538–5559 (2014).
- Vallis, G. K., Zurita-Gotor, P., Cairns, C. & Kidston, J. Response of the large-scale structure of the atmosphere to global warming. *Q. J. R. Meteorol. Soc.* **141**, 1479–1501 (2014).
- Butler, A. H., Thompson, D. W. J. & Heikes, R. The steady-state atmospheric circulation response to climate change-like thermal forcings in a simple general circulation model. *J. Clim.* **23**, 3474–3496 (2010).
- Mbengue, C. & Schneider, T. Storm track shifts under climate change: what can be learned from large-scale dry dynamics. *J. Clim.* **26**, 9923–9930 (2014).



54. Lu, J., Sun, L., Wu, Y. & Chen, G. The role of subtropical irreversible PV mixing in the zonal mean circulation response to global-warming like thermal forcing. *J. Clim.* **27**, 2297–2316 (2014).
55. Harvey, B. J., Shaffrey, L. C. & Woollings, T. J. Deconstructing the climate change response of the Northern Hemisphere wintertime storm tracks. *Clim. Dynam.* **45**, 2847–2860 (2015).
56. Deser, C., Tomas, R. A. & Sun, L. The role of ocean–atmosphere coupling in the zonal-mean atmospheric response to Arctic sea ice loss. *J. Clim.* **28**, 2168–2186 (2015).
57. Held, I. M. & Soden, B. J. Robust responses of the hydrological cycle to global warming. *J. Clim.* **19**, 5686–5699 (2006).
58. Hwang, Y.-T. & Frierson, D. M. W. Corrigendum to Held and Soden (2006). *J. Clim.* **24**, 1569–1560 (2011).
59. O’Gorman, P. A. Understanding the varied response of the extratropical storm tracks to climate change. *Proc. Natl Acad. Sci. USA* **107**, 19176–19180 (2010).
60. Shaw, T. A. & Voigt, A. Tug of war on the summertime circulation between radiative forcing and sea surface warming. *Nature Geosci.* **8**, 560–566 (2015).
61. Simpson, I. R., Shaw, T. A. & Seager, R. A diagnosis of the seasonally and longitudinally varying midlatitude circulation response to global warming. *J. Atmos. Sci.* **71**, 2489–2515 (2014).
62. Chang, E. K. M., Guo, Y. & Xia, X. CMIP5 multimodel ensemble projection of storm track change under global warming. *J. Geophys. Res.-Atmos.* **117**, D23118 (2012).
63. Chang, E. K. M., Zheng, C., Lanigan, P., Yau, M. & Neelin, J. D. Significant modulation of variability and projected change in California winter precipitation by extratropical cyclone activity. *Geophys. Res. Lett.* **42**, 5983–5991 (2015).
64. Zappa, G., Shaffrey, L. C., Hodges, K. I., Sansom, P. G. & Stephenson, D. B. A multimodel assessment of future projections of the North Atlantic and European extratropical cyclones in the CMIP5 climate models. *J. Clim.* **26**, 5846–5862 (2013).
65. Hoskins, B. J. & Woollings, T. Persistent extratropical regimes and climate extremes. *Curr. Clim. Change Rep.* **1**, 115–124 (2015).
66. Woollings, T. Dynamical influences on European climate: an uncertain future. *Phil. Trans. R. Soc. A* **368**, 3733–3756 (2010).
67. Pfahl, S., O’Gorman, P. A. & Singh, M. S. Extratropical cyclones in idealized simulations of changed climates. *J. Clim.* **28**, 9373–9392 (2015).
68. Christensen, J. H. *et al.* in *Climate Change 2013: The Physical Science Basis* (eds Stocker, T. F. *et al.*) Ch. 14 (IPCC, Cambridge Univ. Press, 2014).
69. Willison, J., Robinson, W. A. & Lackmann, G. M. North Atlantic storm-track sensitivity to warming increases with model resolution. *J. Clim.* **28**, 4513–4524 (2015).
70. Emori, S. & Brown, S. J. Dynamic and thermodynamic changes in mean and extreme precipitation under changed climate. *Geophys. Res. Lett.* **32**, L17706 (2005).
71. O’Gorman, P. A. & Schneider, T. The physical basis for increases in precipitation extremes in simulations of 21st-century climate change. *Proc. Natl Acad. Sci. USA* **106**, 14773–14777 (2009).
72. Lu, J. *et al.* The robust dynamical contribution to precipitation extremes in idealized warming simulations across model resolutions. *Geophys. Res. Lett.* **41**, 2971–2978 (2014).
73. Bindoff, N. L. *et al.* in *Climate Change 2013: The Physical Science Basis* (eds Stocker, T. F. *et al.*) Ch. 10.6 (IPCC, Cambridge Univ. Press, 2014).
74. Schneider, T., Bischoff, T. & Plotka, H. Physics of changes in synoptic midlatitude temperature variability. *J. Clim.* **28**, 2312–2331 (2015).
75. Gastineau, G. & Soden, B. J. Model projected changes of extreme wind events in response to global warming. *Geophys. Res. Lett.* **36**, L10810 (2009).
76. Deser, C., Phillips, A., Bourdette, V. & Teng, H. Uncertainty in climate change projections: the role of internal variability. *Clim. Dynam.* **38**, 527–546 (2012).
77. Collins, M. *et al.* Quantifying future climate change. *Nature Clim. Change* **2**, 403–409 (2012).
78. Booth, J. F., Wang, S. & Polvani, L. M. Midlatitude storms in a moister world: lessons from idealized baroclinic life cycle experiments. *Clim. Dynam.* **41**, 787–802 (2013).
79. O’Gorman, P. A. The effective static stability experienced by eddies in a moist atmosphere. *J. Atmos. Sci.* **68**, 75–90 (2011).
80. Schneider, T., O’Gorman, P. A. & Levine, X. J. Water vapor and the dynamics of climate changes. *Rev. Geophys.* **48**, RG3001 (2010).
81. Houze, R. A. Jr *Cloud Dynamics* (Academic, 2014).
82. Field, P. R. & Wood, R. Precipitation and cloud structure in midlatitude cyclones. *J. Clim.* **20**, 233–254 (2007).
83. Allan, R. P. Combining satellite data and models to estimate cloud radiative effect at the surface and in the atmosphere. *Meteorol. Appl.* **18**, 324–333 (2011).
84. Slingo, A. & Slingo, J. M. The response of a general circulation model to cloud longwave radiative forcing. I: Introduction and initial experiments. *Q. J. R. Meteorol. Soc.* **114**, 1027–1062 (1988).
85. Li, Y., Thompson, D. W. & Bony, S. The influence of atmospheric cloud radiative effects on the large-scale atmospheric circulation. *J. Clim.* **28**, 7263–7278 (2015).
86. Ceppi, P. & Hartmann, D. L. Connections between clouds, radiation, and midlatitude dynamics: a review. *Curr. Clim. Change Rep.* **1**, 94–102 (2015).
87. Li, Y., Thompson, D. W., Huang, Y. & Zhang, M. Observed linkages between the Northern Annular Mode/North Atlantic Oscillation, cloud incidence, and cloud radiative forcing. *Geophys. Res. Lett.* **41**, 1681–1688 (2014).
88. Grise, K. M. & Polvani, L. M. Southern Hemisphere cloud-dynamics biases in CMIP5 models and their implications for climate projections. *J. Clim.* **27**, 6074–6092 (2014).
89. Shepherd, T. G. Atmospheric circulation as a source of uncertainty in climate change projections. *Nature Geosci.* **7**, 703–708 (2014).
90. Voigt, A. & Shaw, T. A. Circulation response to warming shaped by radiative changes of clouds and water vapour. *Nature Geosci.* **8**, 102–106 (2015).
91. Ceppi, P. & Hartmann, D. L. Clouds and the atmospheric circulation response to warming. *J. Clim.* **29**, 783–799 (2016).
92. Weatherald, R. T. & Manabe, S. Cloud feedback processes in a general circulation model. *J. Atmos. Sci.* **45**, 1397–1416 (1988).
93. Held, I. M. The gap between simulation and understanding in climate modeling. *Bull. Am. Meteorol. Soc.* **86**, 1609–1614 (2005).
94. Blackburn, M. & Hoskins, B. J. Context and aims of the aqua-planet experiment. *J. Meteorol. Soc. Jpn* **91A**, 1–15 (2013).
95. Philips, N. A. The general circulation of the atmosphere: a numerical experiment. *Q. J. R. Meteorol. Soc.* **82**, 123–164 (1956).
96. Held, I. M. & Suarez, M. J. A proposal for the intercomparison of the dynamical cores of atmospheric general circulation models. *Bull. Am. Meteorol. Soc.* **75**, 1825–1830 (1994).
97. Frierson, D. M. W., Held, I. M. & Zurita-Gotor, P. A gray-radiation aquaplanet moist GCM. Part I: Static stability and eddy scale. *J. Atmos. Sci.* **63**, 2548–2566 (2006).
98. O’Gorman, P. A. & Schneider, T. The hydrological cycle over a wide range of climates simulated with an idealized GCM. *J. Clim.* **21**, 3815–3832 (2008).
99. Kinter, J. L. *et al.* Revolutionizing climate modeling with Project Athena. *Bull. Am. Meteorol. Soc.* **94**, 231–245 (2013).
100. Hanley, J. & Caballero, R. Objective identification and tracking of multicentre cyclones in the ERA-interim reanalysis dataset. *Quart. J. R. Meteorol. Soc.* **138**, 612–625 (2012).

## Acknowledgements

T.A.S. and A.V. are supported by the David and Lucile Packard Foundation. T.A.S. is supported by the Alfred P. Sloan Foundation. We acknowledge support from the National Science Foundation (T.A.S., AGS-1538944; P.A.O., AGS-1148594; E.A.B., AGS-1419818). The National Center for Atmospheric Research is also supported by the National Science Foundation. Y.T.H. is supported by the Ministry of Science and Technology of Taiwan (104-2111-M-002-005). C.I.G. is supported by Israel Science Foundation (1558/14). C.L. is supported by Research Council of Norway project jetSTREAM (231716). We thank participants of the World Climate Research Program’s Stratosphere–troposphere processes and their Role in Climate Workshop on the Storm Tracks. We thank S. Pfahl for Fig. 2 and the reviewers whose comments helped to significantly improve the submitted manuscript.

## Additional information

Reprints and permissions information is available online at [www.nature.com/reprints](http://www.nature.com/reprints). Correspondence should be addressed to T.A.S.

## Competing financial interests

The authors declare no competing financial interests.

## Methods

ERA-Interim calculations of eddy transports were carried out using six-hourly instantaneous data on 18 pressure levels from 1,000 hPa to 10 hPa after filtering with a ten-day high-pass Lanczos filter with 181 weights. DJF and JJA averages from 1980 to 2013 are shown in Fig. 1 for the Northern Hemisphere

and Southern Hemisphere, respectively. Individual extratropical cyclone tracks are identified using the method of ref. 100 applied to six-hourly ERA-Interim sea level pressure. Track density is defined as the number of tracks crossing a spherical cap of 564 km radius ( $10^6$  km<sup>2</sup> area) per season.